Biochimica et Biophysica Acta 1828 (2013) 479–490

Contents lists available at SciVerse ScienceDirect

Biochimica et Biophysica Acta

journal homepage: www.elsevier.com/locate/bbamem

# A conserved interdomain communication pathway of pseudosymmetrically distributed residues affects substrate specificity of the fungal multidrug transporter Cdr1p

Marcin Kolaczkowski [a,*], Kamila Środa-Pomianek [a], Anna Kolaczkowska [b], Krystyna Michalak [a]

[a] Department of Biophysics, Wroclaw Medical University, PL-50-368 Wroclaw, Poland
[b] Department of Biochemistry, Pharmacology and Toxicology, Wroclaw University of Environmental and Life Sciences, ul. Norwida 31, 50-375 Wroclaw, Poland

ARTICLE INFO

*Article history:*
Received 7 May 2012
Received in revised form 19 September 2012
Accepted 21 October 2012
Available online 31 October 2012

*Keywords:*
ABC transporter
Azole antifungal
Mutagenesis
Statistical coupling analysis
Coevolution
Allosteric interaction

ABSTRACT

Understanding the communication pathways between remote sites in proteins is of key importance for understanding their function and mechanism of action. These remain largely unexplored among the pleiotropic drug resistance (PDR) representatives of the ubiquitous superfamily of ATP-binding cassette (ABC) transporters. To identify functionally coupled residues important for the polyspecific transport by the fungal ABC multidrug transporter Cdr1p a new selection strategy, towards increased resistance to a preferred substrate of the homologous Snq2p, was applied to a library of randomly generated mutants. The single amino acid substitutions, located pseudosymmetrically in each domain of the internally duplicated protein: the H-loop of the N-terminal nucleotide binding domain (NBD1) (C363R) and in the C-terminal NBD2 region preceding Walker A (V885G). The central regions of the first transmembrane helices 1 and 7 of both transmembrane domains were also affected by the G521S/D and A1208V substitutions respectively. Although the mutants were expressed at a similar level and located correctly to the plasma membrane, they selectively affected transport of multiple drugs, including azole antifungals. The synergistic effects of combined mutations on drug resistance, drug dependent ATPase activity and transport support the view inferred from the statistical coupling analysis (SCA) of aminoacid coevolution and mutational analysis of other ABC transporter families that these residues are an important part of the conserved, allosterically coupled interdomain communication network. Our results shed new light on the communication between the pseudosymmetrically arranged domains in a fungal PDR ABC transporter and reveal its profound influence on substrate specificity.



## 1. Introduction

ABC transporters constitute a major and ubiquitous protein superfamily controlling the membrane translocation of a large number of structurally diverse solutes ranging from low molecular weight molecules to large polymers including proteins [1]. Many prokaryotic and eukaryotic ABC transporters are involved in the control of membrane permeation to compounds used in the chemotherapy of bacterial and fungal infections and cancer [2–4]. Overproduction of the polyspecific multidrug resistance (MDR) ABC transporters is the prevailing mechanism of resistance to antifungals.

Cdr1p is the major MDR ABC transporter conferring resistance to azoles and other structurally unrelated compounds in the most frequent human fungal pathogen *Candida albicans* [5]. In the related model yeast *Saccharomyces cerevisiae* a similar role is played by the homologous Pdr5p, which shows an overlapping yet distinct specificity with the closely related Snq2p [6].

These transporters are representatives of the Pleiotropic Drug Resistance (PDR) subfamily of ABC transporters classified to two different clusters A (Cdr1, Pdr5p) and D (Snq2p) based on recent phylogenetic analyses [7,8]. Interestingly PDR subfamily members are unique to fungi and plants [9–13]. Their characteristic feature, in contrast to other ABC superfamily members including mammalian P-glycoproteins involved in cancer cell chemotherapy resistance, is the inverted topology. The minimal functional unit believed to operate in most ABC transporters is a symmetrically arranged tandem repeat of the nucleotide binding (NBD) and transmembrane domains (TMD): TMD1–NBD1–TMD2–NBD2, which in the PDR subfamily shows the mirror image organization: NBD1–TMD1–NBD2–TMD2 [14–16].

The observed two-fold molecular symmetry of domain arrangement, resulting from the internal duplication is implied, according to the alternating access model, to have important consequences for the mechanism of drug transport and harnessing energy from ATP-hydrolysis. Its mutational analysis by a rational approach is hindered by the scarce

*Abbreviations:* MDR, multidrug resistance; PDR, pleiotropic drug resistance; ABC, ATP-binding cassette; NBD, nucleotide binding domain; TMD, transmembrane domain; TM, transmembrane; SCA, statistical coupling analysis; 4-NQO, 4-nitroquinoline 1-oxide; $DiOC_6$, 3,3′-dihexyloxacarbocyanine iodide

* Corresponding author at: Department of Biophysics, Wroclaw Medical University, Chalubinskiego 10, PL-50-368 Wroclaw, Poland. Tel.: +48 71 7841403; fax: +48 71 7840088.
*E-mail address:* mkolacz2@poczta.onet.pl (M. Kolaczkowski).

0005-2736/$ – see front matter © 2012 Elsevier B.V. All rights reserved.
http://dx.doi.org/10.1016/j.bbamem.2012.10.024

structural information, which in the case of fungal-type PDR ABC transporters is limited to low resolution single particle analysis of Pdr5p [17], as well as the usually observed large sequence divergence of the duplicated subunits.

In the PDR-subfamily these are encoded as a single polypeptide, in which even the consensus regions of C-loop, Walker A and the H-loop of the two NBDs contain substitutions of the critical and highly conserved amino acid residues [7,8] and are not interchangeable [18].

Such degeneracy is not limited to the PDR subfamily. It has also been observed in other ABC proteins, such as the human Tap complex involved in the presentation of antigenic peptides in the immune system, the CFTR chloride channel whose defects lead to cystic fibrosis, the multidrug resistance associated protein MRP1 and the subunit of the ATP-sensitive potassium channel regulating insulin release SUR1, suggesting a functional nonequivalence of the two NBDs [19–23]. In CFTR a prolonged binding of ATP occurs at the NBD1 site, whereas its rapid turnover and hydrolysis at the NBD2 site is coupled to chloride channel gating [20]. Based on this functional nonequivalence, reflected by a large sequence divergence, possible mechanistic differences with transporters having the critical regions conserved in both halves, such as P-glycoprotein have been postulated [21,24]. In P-glycoprotein ATP hydrolysis at both NBDs occurring in an alternating fashion was required for drug transport [25,26] and even the complete substitution of the C-terminal NBD by the N terminal one resulted in a transport capable chimera [27].

Intriguingly however, despite the structural differences the representatives of the fungal-type PDR subfamily of ABC transporters Pdr5p and Cdr1p, share with mammalian P-glycoproteins many common substrates and inhibitors implying some functional and mechanistic similarities. Crucial for their understanding is uncovering of the functional coupling between selected residues important for the long distance interdomain allosteric interactions. These, shown to operate in other protein families and to impact their substrate specificity [28–31], are poorly understood in the members of the ubiquitous ABC superfamily. A light on these complex interdomain interactions has been shed by the recent analysis of the *S. cerevisiae* Pdr5p mutants, which revealed communication between transmembrane helix 2 and the Q loop region of NBD1 with the involvement of intracellular loop 1 [32,33].

Our results build on the previous extensive characterization of drug specificity profiles of yeast PDR transporters [6,34]. This allowed for the design of a new *in vivo* selection procedure of randomly generated Cdr1p gain of function mutants, that conferred increased level of resistance towards specific substrates of the homologous Snq2p. Interestingly the analysis reveals a pseudosymmetrical location of residues involved in communication between substrate and nucleotide binding domains and selectively affecting transport specificity.

## 2. Materials and methods

### 2.1. Strains and media

The following yeast strains were used in this study: AK100 (MATa, ura3-52, trp1Δ63, leu2Δ1, his3Δ200, GAL2+, PDR1–3, pdr5-Δ4::rep500, snq2-Δ1::hisG, yor1-1::hisG), MKCDR1h (MATa, ura3–52, trp1Δ63, leu2Δ1, his3Δ200, GAL2+, PDR1–3, pdr5-Δ4::CDR1h, snq2-Δ1::hisG, yor1-1::hisG), MKSNQ2h (MATa, ura3–52, trp1Δ63, leu2Δ1, his3Δ200, GAL2+, PDR1–3, pdr5-Δ4::SNQ2h, snq2-Δ1::hisG, yor1-1::hisG) [34], cells were grown on rich YPD or on synthetic complete medium lacking the relevant auxotrophic components.

### 2.2. Random mutagenesis, selection, subcloning and chromosomal integration of the mutant alleles

The pMKCDR1h plasmid [34] was treated with hydroxylamine as described previously [35]. After transformation into AK100, cells were plated on resazurine containing synthetic complete medium lacking uracil, supplemented with 2% glycerol and 2% ethanol. The drug resistance phenotypes of mutant plasmids were verified after isolation from streak-purified colonies and retransformation into AK100. The sequence of the resulting clones bearing single point mutations was determined by the Sanger dideoxy chain termination procedure [36].

Combined mutations were generated by subcloning of the corresponding fragments with restriction endonucleases, using standard procedures. The presence of mutations, resulting either in the loss or gain of an additional restriction endonuclease site, was confirmed by agarose gel electrophoresis after digestion of the whole plasmid or its PCR-amplified fragments.

The chromosomal integration of mutant alleles, was achieved by transformation of the isolated linear fragments, containing the entire *CDR1* open reading frame flanked by the promoter and terminator regions of *PDR5*, into the AK100 strain, essentially as previously described [34]. The resulting clones were verified by colony PCR and sequencing.

Susceptibility of yeast to growth inhibition was determined as previously described [34]. At least four independently isolated clones were compared in the growth assays of drug resistance. The drug resistance profiles of the representative integrants were in agreement with those obtained with plasmid transformants.

### 2.3. Plasma membrane isolation

Isolation of plasma membranes was performed according to the glass-bead lysis procedure [37], with minor modifications [38]. Membranes were analyzed by sodium dodecyl sulfate (SDS)-polyacrylamide gel electrophoresis and stained with Coomassie brilliant blue R-250 (Bio Rad).

### 2.4. Immunological methods

Protein extracts were prepared and the protein concentration was determined as previously described [39]. After separation of equal protein amounts by SDS-PAGE and transfer, blots were incubated with India HisProbe-HRP (Pierce) and anti-Vph1p antibody (Molecular Probes). Blots were developed with the SuperSignal West Pico chemiluminescent substrate (Pierce).

### 2.5. Transport and ATPase activity measurements

The accumulation of resorufin acetate (Fluka) was measured under similar conditions to those described previously [34]. Briefly, the reaction was started by addition of resorufin acetate to energized cells collected during the exponential phase of growth. Fluorescence intensity was recorded with a Molecular Devices Gemini EM microplate spectrofluorometer at 544 nm excitation and 590 nm emission wavelengths.

Measurements of ATPase activity were performed essentially as previously described [37], with minor modifications. Briefly, plasma membranes were suspended in 100 mM buffer of desired pH. The reactions were started by addition of $MgCl_2$ and ATP and carried at 30 °C. After termination at multiple time points, to assure linearity, the concentration of liberated inorganic phosphate was determined as described previously [37]. To optimize conditions, the ATPase pH profiles were determined in Mes-NaOH (pH 5.5; 6; 6.5), Mops-NaOH (pH 6.5; 7), Hepes-NaOH (pH 7; 7.5; 8), Taps-NaOH (pH 8; 8.5; 9) in the presence or absence of several metabolic inhibitors including oligomycin (12.5 μg/ml ) (inhibitor of Cdr1p and the mitochondrial ATPase), vanadate (50 μM) (inhibitor of Cdr1p and Pma1p) sodium azide (12.5 mM) (inhibitor of mitochondrial ATPase), nitrate (50 mM) (inhibitor of vacuolar ATPase) and ammonium molybdate (200 μM) (inhibitor of non-specific phosphatases). Membranes from the expression host not containing Cdr1p were used as an additional negative control. The vanadate sensitive, oligomycin insensitive Pma1p activity was used as a positive control to monitor the quality of membrane preparations. The pH ranges of buffers overlapped to monitor possible indirect effects of

buffers on the activity. As no effect of nitrate and molybdate was observed, the effects of Cdr1p drug substrates were routinely performed in 100 mM Hepes pH 7.5, supplemented with 12.5 mM sodium azide at saturating Mg-ATP concentrations (8 mM).

$DiOC_6$ transport in isolated plasma membranes was measured under similar conditions to those described previously for rhodamine 6 G transport by Pdr5p [34,38] with minor modifications: the reaction buffer contained 100 mM Hepes pH 7.5 and 12.5 mM sodium azide, excitation and emission wavelengths were 485 nm and 510, respectively. Reactions were started by addition of $MgCl_2$ and ATP (8 mM final concentration unless indicated differently) and carried at 30 °C.

### 2.6. Computational analysis of amino acid coevolution and structural visualization

The statistical coupling analysis (SCA) [40] was performed, with the help of the integrated system for residue coevolution [41]. The analysis of the calculated coevolution perturbation matrix was performed using the previously implemented [42], two dimensional, coupled two way clustering procedure [43,44]. Data were visualized with the help of Java Treeview [45] and MeV [46].

The input multiple alignment was generated with MUSCLE [47] on a large representative set of 600 homologous sequences retrieved from the BLAST search of the available non-redundant protein sequences.

An Expresso (3D-Coffee) multiple sequence alignment (MSA) [48] was performed based on the structures of NBD domains of ABC proteins available from the Protein Data Bank. The prediction of secondary structure was performed by PORTER [49] and that of transmembrane helices by the SPLIT 4.0 server [50].

Molecular graphics images were produced using the UCSF Chimera package from the Resource for Biocomputing, Visualization, and Informatics at the University of California, San Francisco (supported by NIH P41 RR001081) [51].

## 3. Results

### 3.1. Pseudosymmetrical distribution of Cdr1p residues important for substrate specificity

To identify residues of Cdr1p important for substrate specificity we took a new approach aiming at the alteration of its resistance profile towards previously identified compounds specifically detoxified by the homologous Snq2p [6]. *Saccharomyces cerevisiae* mutants of increased resistance to resazurine were selected from a pool of approximately 400 000 transformants, containing the library of mutagenized Cdr1p expression plasmid. Thirty-five resistant clones were initially isolated, from which the plasmids were rescued and retransformed into the expression host. The 10 clones remaining after confirmation of plasmid-borne phenotypes and initial characterization of the alterations in the drug resistance profiles were sequenced. This revealed the presence of five single base substitutions in the *CDR1* open reading frame. These resulted in single amino acid substitutions, some occurring in multiple clones, which were pseudosymmetrically located in each domain of the internally duplicated Cdr1p primary structure. The mutations found at the beginning of both TMDs were placed in the corresponding central regions of TM helices 1 and 7 (Fig. 1 A.). Guanine 1561 in the nucleotide sequence was substituted twice by A and G1562 once by A, leading to the exchange of Gly 521 by larger and more polar S or D respectively, located in the central part of TM helix 1, encompassing residues 514–535 of the N-terminal TMD1. The corresponding region of the C-terminal TMD2 was affected in four clones containing the C3623T substitution, leading to the replacement of Ala 1208 by the larger and more hydrophobic Val in the central region of the TM helix 7, encompassing residues 1197–1214 (Fig. 1A).

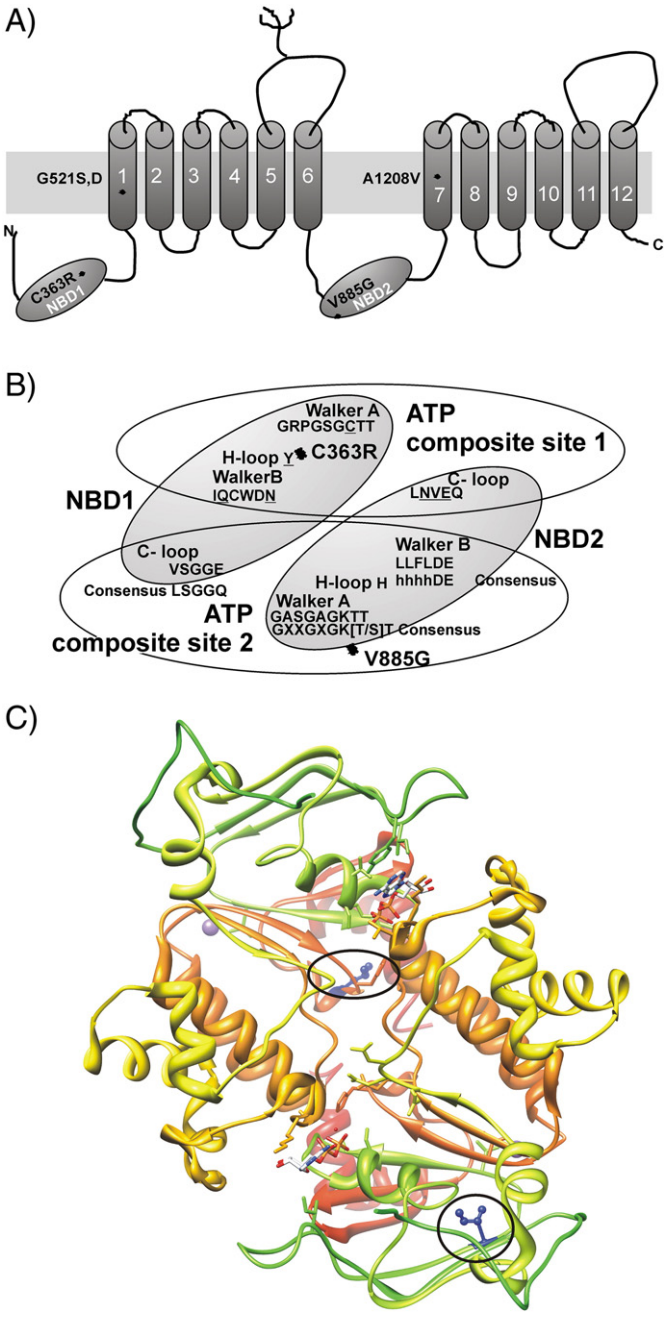


**Fig. 1.** Pseudosymmetrical localization of mutations involved in the switch of Cdr1p substrate specificity towards compounds preferred by Snq2p along the two fold rotational symmetry axis observed in ABC transporters. A) Schematic representation of the primary Cdr1p structure revealing that each of the internally duplicated domains is affected. B) The detailed location of the C363R in the H loop of NBD1, forming the degenerate ATP composite site 1. The V885G lies in the region preceding Walker A of NBD2 in the canonical ATP composite site 2. C) Localization of the corresponding residues L536 and I364 in the nucleotide binding domains of Sav1866 based on structure based multiple sequence alignment and the available atomic coordinates of this homodimer composed of the duplicated TM-NBD subunits of identical primary structure (2HYD). The top view from the TM domain side (removed for clarity) on the dimer of both NBD subunits characterized by a twofold rotational symmetry reflecting the perfect symmetry of the primary structure. The image was generated with UCSF Chimera [51].

Two additional substitutions were located in the NBDs which, in contrast to the TM regions, show high degree of primary structure conservation among ABC transporters. The NBDs form a close contact upon binding of ATP molecules which are sandwiched between the Walker A and B motives and the H-loop of the catalytic domain of one NBD, and the C-loop of the helical signaling domain of the second

NBD. The latter is believed to communicate with the TMDs via the intracellular loops connecting the TM helices. In this way two conformationally coupled composite ATP-binding sites are formed with the contribution of the conserved regions of both NBDs (Fig. 1B) [52,53].

Interestingly the identified mutations of Cdr1p NBDs, influencing substrate specificity, affected both ATP composite sites I and II. One of them, resulting from the T2654G base substitution, leads to the exchange of Val 885 into Gly at the 10th position upstream of the Walker A region of NBD2 within the canonical ATP composite site II (Fig. 2A). In the two remaining clones with the T1087C base substitutions, the corresponding Cys 363 was replaced by the much larger R in the degenerate H-loop region of NBD1. This is the second position downstream of the site usually occupied by the conserved histidine in the majority of ABC transporters, which in the PDR subfamily members has been replaced by Y [7,8] (Fig. 2B).

Given the lack of available crystal structures of Cdr1p and other members of the PDR subfamily, the prediction of the relative location of the identified NBD residues was based on a structure based alignment of the affected regions of Cdr1p and other fungal transporters with the sequences of the crystallized NBD domains deposited in the Protein Data Bank. No gaps were found between the two mutation sites and the conserved Walker A and H-loop motives respectively (Fig. 2A and B), which allowed to map precisely the relative locations of the corresponding residues in NBD domains of known three dimensional structure. A large distance exceeding 30 angstroms separating residues L536 and I364 of the Sav1866 homodimer in the closed conformation, corresponding to C363 and V885 of Cdr1p, respectively is highlighted in Fig. 1C.

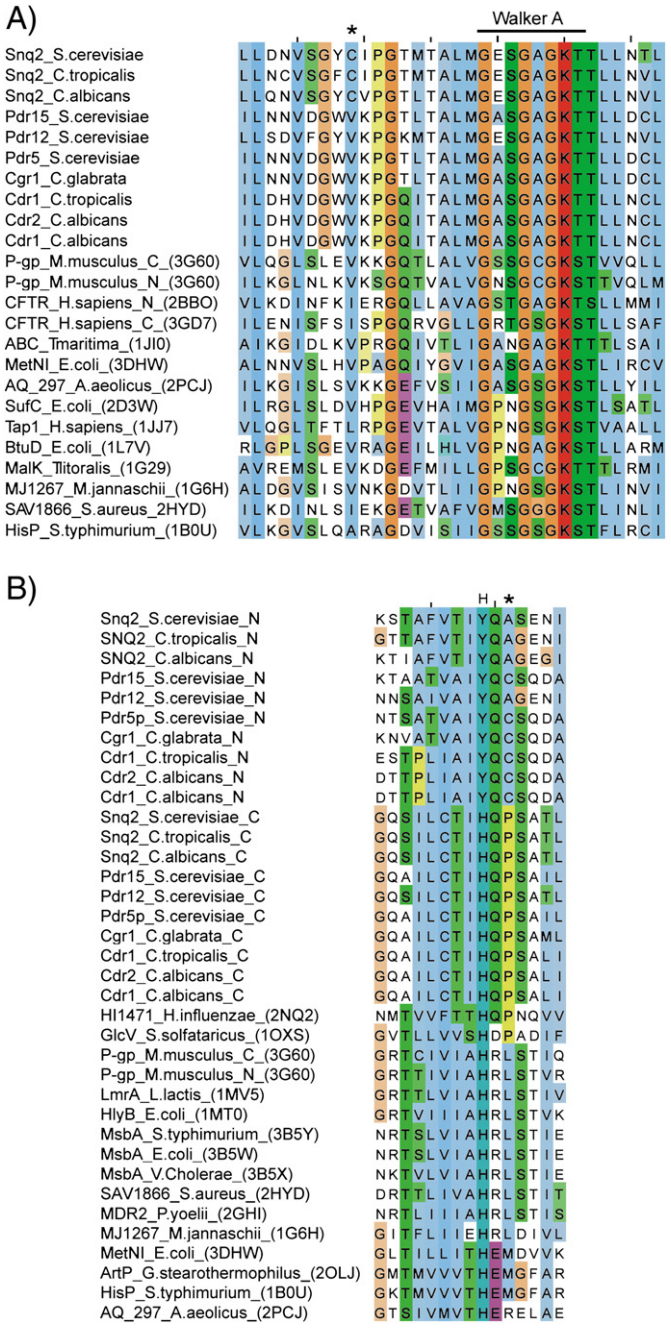


**Fig. 2.** Location of the identified mutations with the help of structure based Expresso (3D-Coffee) multiple sequence alignment of the NBD domains of fungal ABC transporters of the PDR subfamily with NBD domains of other ABC proteins of known 3D structure. A) The aligning region around Walker A motif of selected proteins is shown. The substituted V885 residue of *Candida albicans* Cdr1p NBD2 is marked by a star. B) The H-loop region of the degenerate N-terminal NBD1 affected by the C363R substitution (indicated by the star) and the canonical C-terminal NBD2 of selected fungal PDR ABC transporters (with the conserved histidine indicated by H) is shown.

### 3.2. High level expression of the mutant and wild type Cdr1 alleles

The observed separation of the identified Cdr1p mutations and their common effect on substrates of Snq2p raised the possibility of their synergistic interactions resulting from long distance communication. To verify this, the single and newly generated multiple mutants were stably overproduced after integration into the chromosome at the *PDR5* locus. The expression level of mutant Cdr1p alleles was comparable to that of wild type as revealed by Western blot of whole cell extracts (Fig. 3A). The high and comparable amount of correctly localized mutant and wild type Cdr1p proteins was found in the plasma membrane fractions as revealed by SDS PAGE analysis of the isolated fractions (Fig. 3B).

### 3.3. Changes in drug resistance and transport indicate functional coupling of the identified residues involved in substrate specificity

Analysis of the drug resistance profiles revealed selective changes associated with the identified Cdr1p mutations. As expected, all the single mutants showed an increase in resistance to resazurine (Fig. 4A).

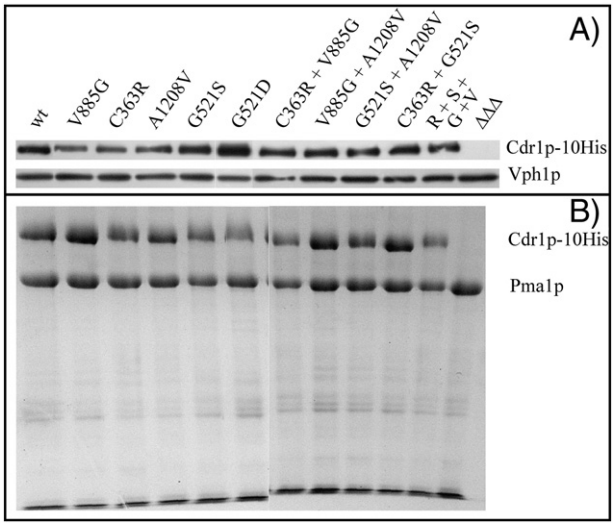


**Fig. 3.** Expression level of the overproduced Cdr1 wild type and single and multiple mutant alleles. A) Western Blot of whole cell extracts. B) Coomasie stained SDS PAGE of isolated plasma membranes. The positions of the Cdr1p band is indicated. Vph1p band serving as a loading control is visualized. The position of the marker enzyme of the yeast plasma membrane Pma1p is indicated. The extracts of the quadruple mutant C363R, G521S, V885G, A1208V (R + S + G + V) and the expression host bearing the triple deletion in *PDR5*, *SNQ2* and *YOR1* (ΔΔΔ) are indicated.

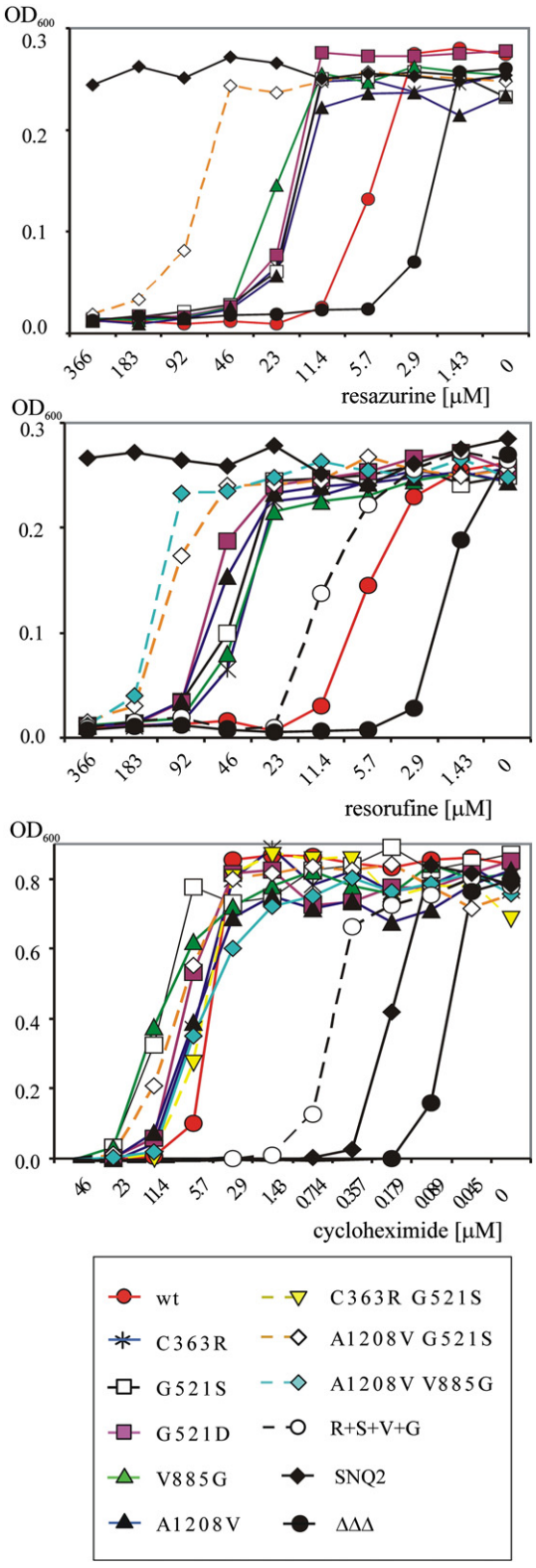


**Fig. 4.** Altered drug resistance profiles of the single and multiple Cdr1p mutants. Serial dilutions of indicated drugs in liquid growth medium (supplemented either with glycerol and ethanol for resazurine and resorufine or glucose for cycloheximide) were prepared in microtiter plates. Growth was monitored by optical density measurements and visual inspection. The mean values of at least three independent experiments are presented. Error bars have been omitted for clarity.

An even higher, about eightfold increase in resistance to a structurally similar specific Snq2p substrate resorufine was observed, as compared to wild type Cdr1p, which conferred only low level-resistance to both compounds (Fig. 4B). To verify that the associated changes in resistance correspond to the increased transport activity of Cdr1p mutants, a new fluorescence based assay was developed with the profluorochrome resorufin acetate as the substrate. A rapid intracellular accumulation of this compound associated with the release of resorufin fluorescence, by the activity of nonspecific cytosolic esterases, was observed in the case of the expression host strain, in which the genes encoding the major MDR transporters *PDR5*, *SNQ2* and *YOR1* have been deleted (Fig. 5).

Overproduction of Snq2p completely blocked resorufin acetate accumulation, and in this case the fluorescence trace was similar to the cell free buffer control. Although the decrease of resorufin acetate accumulation observed upon Cdr1p overproduction was much smaller than in the case of Snq2p, a marked decrease was observed in the mutants (Fig. 5). This was in line with the results of the growth assay, indicating that the mutants are more effective in the extrusion of resorufin acetate as compared to the wild type Cdr1p. No differences in the rates of fluorescence increase were observed upon contact of resorufin acetate with glass bead-generated extracts of the analyzed strains, which confirmed that the differences observed with whole cells result from alterations of permeation due to changes in active extrusion.

Analysis of the drug related phenotypes of the double Cdr1p mutants to Snq2p-specific substrates revealed an even higher increase in resazurine resistance, specifically resulting from the combination of G521S and A1208V substitutions (Fig. 4A), indicating the functional coupling of both TMD residues. This double mutant exerted also an increased resistance to another Snq2p substrate 4-NQO (not shown). In contrast, the combined NBD mutations C363R and V885G conferred the same level of resazurine resistance as the corresponding single mutants (omitted for clarity in Fig. 4). The same was observed on resorufine where also the double V885G, A1208V mutant showed the highest increase in resistance, similar to that exhibited by the G521S, A1208V combination. An intermediate increase in resistance to resazurine was observed for the V885G, A1208V as well as the C363R, G521S double mutants as compared to single substitutions (omitted for clarity in Fig. 4). The quadruple C363R, G521S, V885G and A1208V mutation abolished the stimulatory effect of the analyzed single and double mutants, diminishing the resorufine (Fig. 4B) and resazurine (omitted for clarity in Fig. 4) resistance to the low level observed with wild type Cdr1p.

In contrast to Snq2p-specific substrates, no further increase in resistance to cycloheximide, which is a preferred substrate of Pdr5p and Cdr1p, was observed in double mutants, although all single ones showed a slight increase (Fig. 4C). Importantly the C363R, G521S,

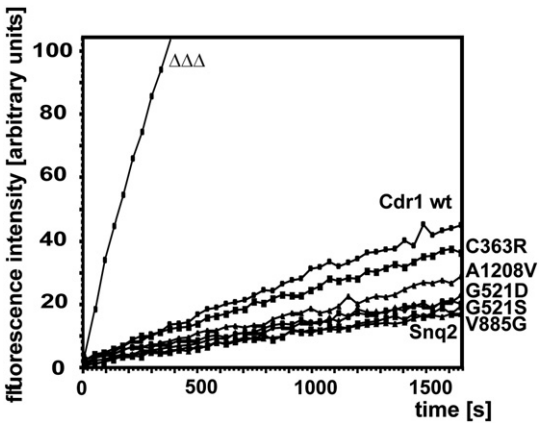


**Fig. 5.** Transport of resorufin acetate by wild type Cdr1p and the mutants. The increase in fluorescence intensity is proportional to the level of intracellular accumulation of the profluorochrome and the release of free resorufin by nonspecific esterases. A decrease in the reaction rate indicates increased extrusion by the mutants. The signal from the Snq2p overproducing strain, which is similar to the cell free buffer control is also indicated.

V885G, A1208V quadruple mutant almost completely lost the ability to confer cycloheximide tolerance (Fig. 4C).

### 3.4. Combined mutations lead to strong synergistic effects on selected azole antifungals

Azoles are an important class of synthetic molecules widely used in the treatment of human fungal infections and crop protection in agriculture. They are transported ligands of both the fungal PDR subfamily members, as well as the mammalian ABC proteins, such as the P-glycoprotein [54,55], although differences in selectivity exist among these transporters. The analysis of azole interactions with the isolated mutants revealed a strong and selective reduction of resistance to itraconazole, associated with the C363R substitution in the H-loop of NBD1. A gradual decrease of itraconazole resistance upon increasing size and polarity of the residue occupying position 521 in TM1 was also observed with the G521S and D mutants (Table 1). In contrast these mutations showed no (C363R, G521S) or only slight decrease (G521D) of resistance to the structurally related, but smaller in size ketoconazole, which is a good substrate of both Cdr1p and Snq2p [34]. The G521D mutation was also associated with the reduced level of resistance to other azoles, such as fenbuconazole (Table 1). In contrast resistance of the G521S and D mutants to fluconazole was slightly elevated as compared to the wild type Cdr1p (Table 1). These data indicate the strong and selective influence of the identified NBD and TMD residues on azole transport specificity.

Whereas the combined double mutations had only a small effect on resistance to fluconazole and ketoconazole, the strong synergistic decrease of resistance to fenbuconazole by the double C363R-G521S, C363R-V885G, A1208V-G521S and A1208V-V885G mutants was observed (Table 1). A similar synergy was observed with itraconazole. The strongest effect was observed with the quadruple mutant C363R, G521S, V885G, A1208V, which showed a markedly reduced activity towards the four azoles as compared to the single mutants and the wild type Cdr1p. This underscores the importance of the interactions between the identified residues for drug translocation, and together with the synergistic effects observed on resazurine, resorufine, 4-NQO and selected azoles, indicates their functional coupling.

### 3.5. Coevolutionary analysis of the residue interactions in the PDR subfamily of ABC transporters

Recent evidence suggests that conformational changes in proteins depend on proper long distance communication between remote amino acids through evolutionarily conserved contacts established in the form of a sparse network of selected intermediary residues [40,42]. To get more insight into the interaction network in Cdr1p, and the function of the newly identified residues, we used new methods that allow predicting the degree of thermodynamic coupling between protein residues, which have successfully been applied to map the interactions in several protein families and verified by mutagenesis [40,42,56]. These are based on the fact that substitutions of the functionally important residues showing some degree of conservation are often compensated by changes at other positions. As a consequence of such coevolutionary events, the distribution of amino acids occupying a given position in the large MSA changes in the subalignment containing a specific substitution (perturbation) at another site [42]. The magnitude of this change, reflecting the energetic coupling of residue pairs can be calculated and presented in the form of a color-coded two dimensional matrix, which for the PDR subfamily is presented in Fig. 6A. This reveals the pseudosymmetrical pattern of interactions, reflecting, the two fold rotational symmetry typically observed in structures of ABC transporters, including the three dimensional, low resolution reconstruction of Pdr5p [17] and important sequence differences between the duplicated subunits [7,8]. Functionally linked residues, should be characterized by a similar profile of energetic coupling to other residues in the protein. The identification of such groups has been performed by the subsequent two dimensional clustering analysis of the interaction matrix (Fig. 6B). This led to the identification of V885 as a member of a larger cluster of residues (Fig. 6C) showing self consistency, characterized by a similar pattern of residue coupling to all substitutions (perturbations), and substitutions (perturbations) showing a similar pattern of coupling to all residues. This characteristic feature of related, network-forming residues was previously seen by others [40,42,56].

Interestingly several residues revealed by the two dimensional clustering to be coevolutionarily related to V885 are located in the region of the conserved X-loop [53], that is part of the communication pathway between the NBD and TM domains that shows high mobility in molecular dynamics simulations of ABC exporters [57,58]. These residues include G998 located in the X-loop and A990, which together with G1000 surround this conserved motif from both sides. G1000 immediately precedes the degenerate motif C of NBD2, which is followed by R1006 also belonging to the V885 cluster. Interestingly K483 of Sav1866 corresponding to R1006 of Cdr1p, based on the structure based alignment, has been implicated to be involved in the formation of one of the switches mediating the interdomain communication, in the Sav1866 homodimer [59]. Structure based alignment analysis revealed another residue V952 from the V885 cluster to be located in the proximity of the X-loop region, as a close contact between residues corresponding to A990 and V952 of Cdr1p in the structure based alignment, was observed in the crystal structures of several NBD domains.

Among other functionally important regions of ABC transporters highlighted by the evolutionary coupling to V885 were also the A loop of NBD2 (consensus ATP composite site 2), which based on the structure assisted alignment is in close contact with the residues corresponding to I169 and L170, as well as the region of a loop joining alpha helices 3 and 4 of the signaling subdomain of NBD2, in which residues corresponding to the identified A255, P261, Y273 of Cdr1p are located. In addition several residues located within the predicted loops joining the transmembrane helices were also found in the V885 cluster. Structural analysis of other ABC transporters combined with molecular dynamics simulations suggests that these regions undergo excessive rearrangements and show high mobility during the catalytic cycle [57,58,60,61].

In view of these observations it is also interesting to note the coevolutionary link of the V885 cluster with the central region of TM7 (L1209) also affected in our mutagenesis approach.

**Table 1**
The differential influence of Cdr1 wild type, single and multiple mutants on resistance to azoles.[a]

| | Cdr1 wt | C363R | G521S | G521D | V885G | A1208V | C363R G521S | C363R V885G | A1208V G521S | A1208V V885G | R+S+G+V | Snq2 | ΔΔΔ |
|---|---|---|---|---|---|---|---|---|---|---|---|---|---|
| Fluconazole | 549 | 549 | 1098 | 1098 | 1098 | 1098 | 549 | **274** | 1098 | **549** | ***34*** | 17 | 4.3 |
| Fenbuconazole | >366 | >366 | >366 | 11.4 | >366 | >366 | ***23*** | ***11.4*** | ***46*** | ***92*** | ***2.9*** | 92 | 0.179 |
| Ketoconazole | 1.4 | 1.4 | 1.4 | 0.714 | 5.7 | 5.7 | 1.4 | **0.714** | 2.9 | 2.9 | ***0.179*** | 0.714 | 0.022 |
| Itraconazole | >46 | 2.9 | 11.4 | 0.357 | >46 | >46 | **1.43** | ***0.179*** | ***5.7*** | ***11.4*** | ***0.045*** | 0.089 | 0.022 |

[a] The minimal inhibitory concentrations MIC [μM] are indicated. The increased effect of combined mutations is marked in boldface. A strong synergistic increase is marked in italics. The MIC values for the expression host bearing the triple deletion of the major multidrug transporter genes *PDR5*, *SNQ2* and *YOR1* and the Snq2p overproducing strain are shown for reference.

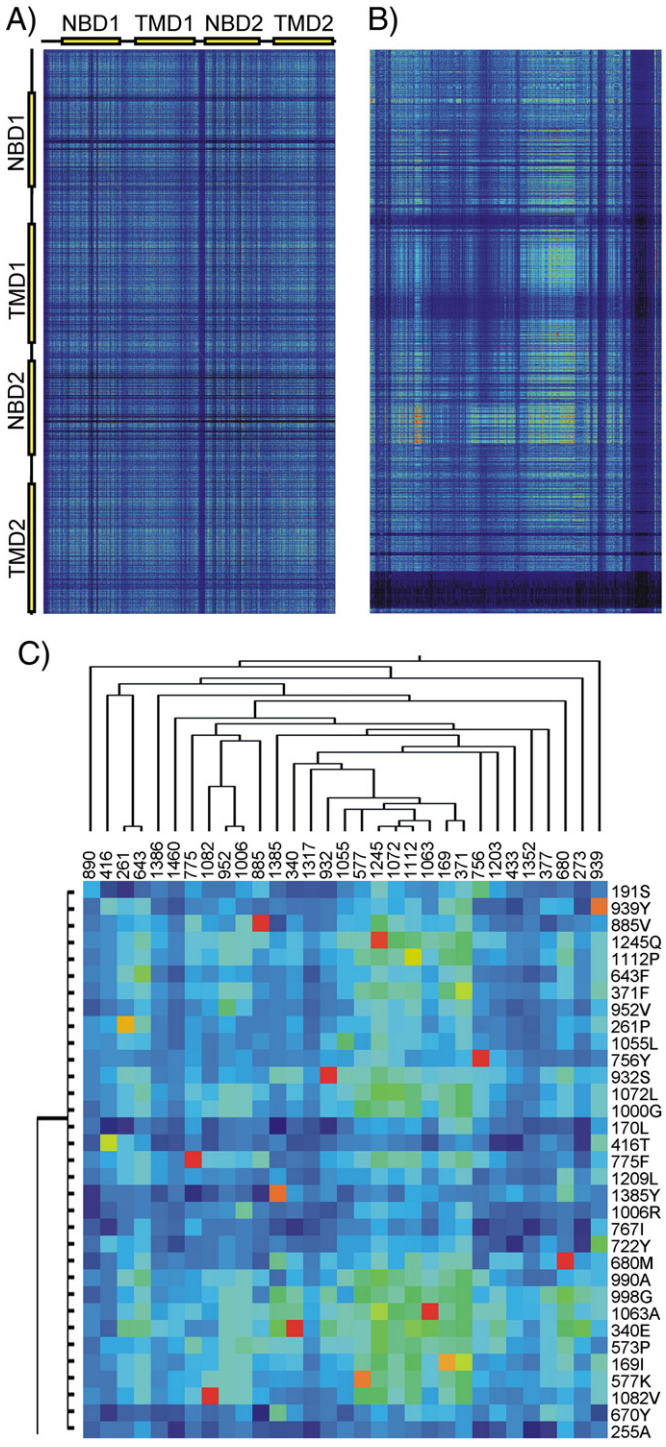


**Fig. 6.** Analysis of statistical coupling in the PDR subfamily of ABC transporters. A) A color coded-matrix of coupling energy values for the 2551 substitution (perturbation) analyses on the MSA as indicated in the text (values increasing from blue, through green and yellow to red). Each row represents coupling energy values for subsequent residues in the alignment (their location in the MSA is indicated by domain symbols on top) in response to a substitution (perturbation) at another position of MSA whose location is indicated by domain symbols on the left side. Each column represents coupling energies for one residue over all substitutions (perturbations). B) The coupling energy matrix after two dimensional clustering, grouping residues showing a similar pattern of coupling energies in response to all substitutions (perturbations) and substitutions (perturbations) showing a similar pattern of coupling to all residues. C) Detailed view of the self consistent cluster of residues identified by two dimensional clustering, coupled to V885 (numbers on top indicate position of the amino acid residue in the Cdr1p sequence). These show a similar pattern of coupling energies in response to substitutions at positions indicated on the right. The indicated substitutions show also a similar pattern of coupling to the residues indicated on top.

### *3.6. The involvement of identified residues in communication between drug and nucleotide binding sites*

ATP hydrolysis is tightly coupled to substrate translocation in the majority of transport systems including representatives of the ABC superfamily, such as HisP [62]. The polyspecific multidrug transporters such as P-glycoprotein are distinct in that respect and show a high level of basal ATPase activity even in the absence of transported drugs. Substrate binding in the TM region of P-glycoprotein is communicated to the NBD domains, which results in the strong stimulation of ATPase activity at low drug concentrations, whereas higher exert an inhibitory effect [63,64].

To verify whether the identified residues interfere with signals elicited by transported drugs, their effect on Cdr1p ATPase activity was analyzed. In agreement with the previous observations on Pdr5p [65–67], the inhibition of Cdr1p by high concentrations of transported substrates was also observed with only a minor or no stimulation at low doses for most compounds (data not shown). The response to fenbuconazole presented in Fig. 7 is interesting as this azole antifungal showed a significant stimulation of the wt Cdr1p ATPase activity, which was markedly enhanced by G521S and G521D mutations in the TM helix 1. In contrast mutations at other three positions had an opposite effect and markedly diminished the stimulation and enhanced inhibition. Interestingly the single C363R substitution was sufficient for almost complete elimination of the substrate drug stimulatory effect on ATPase activity both in the wild type context as well as in the presence of the enhancing G521S substitution, indicating interference with a common path of signal transmission. The effect of single A1208V and V885G mutations was of lower magnitude, however when combined these two substitutions exerted an effect similar to that of a single C363R change. An even stronger inhibitory effect was observed when C363R and V885G mutations were combined, and with the quadruple

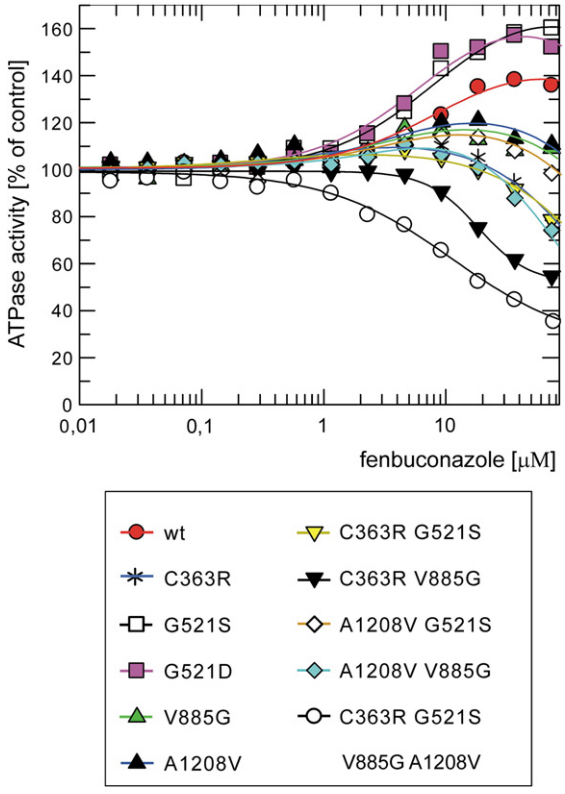


**Fig. 7.** Transported drug-dependent ATPase activity of Cdr1p wild type and mutants in the isolated plasma membranes. Membranes were isolated as described in Materials and methods. ATPase activity was measured at 30 °C, pH 7.5 in the presence of 8 mM Mg-ATP and 12.5 mM azide, as described in Materials and methods.

mutant being particularly prone to inhibition of the ATPase activity by fenbuconazole. These observations extend and further support the long range interactions of the identified residues, observed in growth assays, indicating a coordinated modification of drug elicited signaling to the NBDs.

Whereas the quadruple mutant with markedly decreased capability to confer resistance to all tested substrates was able to hydrolyze ATP at a rate comparable to the wild type Cdr1p at high, saturating concentration of 8 mM, the analysis revealed a reduced rate at lower concentrations associated with a fivefold increase in the $K_M$. This could potentially contribute to decreased drug resistance observed in growth assays as the *in vivo* ATP concentrations are typically in the milimolar range [68,69]. To measure the drug transport activity of this mutant at saturating drug and ATP concentrations, difficult to control *in vivo*, a new fluorescence-based assay of $DiOC_6$ transport in isolated plasma membranes was developed. This lipophilic probe, which is also a transported substrate of Pdr5p and P-glycoprotein, shows enhanced fluorescence upon lipid binding [70,71]. Addition of ATP to Cdr1p overproducing plasma membrane preparation, in the presence of the dye, was followed by a rapid decrease of fluorescence intensity, which was not observed with the control membranes not containing Cdr1p and in the absence of ATP (Fig. 8). In line with the strong inhibition of Cdr1p ATPase activity by oligomycin and vanadate, they also inhibited Cdr1p mediated decrease of $DiOC_6$ fluorescence intensity, when applied before starting the reaction with Mg-ATP. When the inhibitors were added after the reaction has reached a steady state, a rapid restoration of fluorescence was observed. This excludes the possibility that the decrease of fluorescence intensity resulted from degradation or chemical modification of the dye. The results are in line with our previous observations that Cdr1p removes drugs directly from the plasma membrane to the external medium [34]. At low ATP concentrations both ATPase activity and $DiOC_6$ transport of the quadruple mutant were compromised as compared to the wild type. Although the increase of ATP concentration restored the full ATPase activity also observed in the wild type, the transport of $DiOC_6$ showed no increase and was barely detectable. This further supports the results from growth inhibition assays, and SCA analysis demonstrating that ATP hydrolysis is not efficiently coupled to substrate translocation in this mutant.

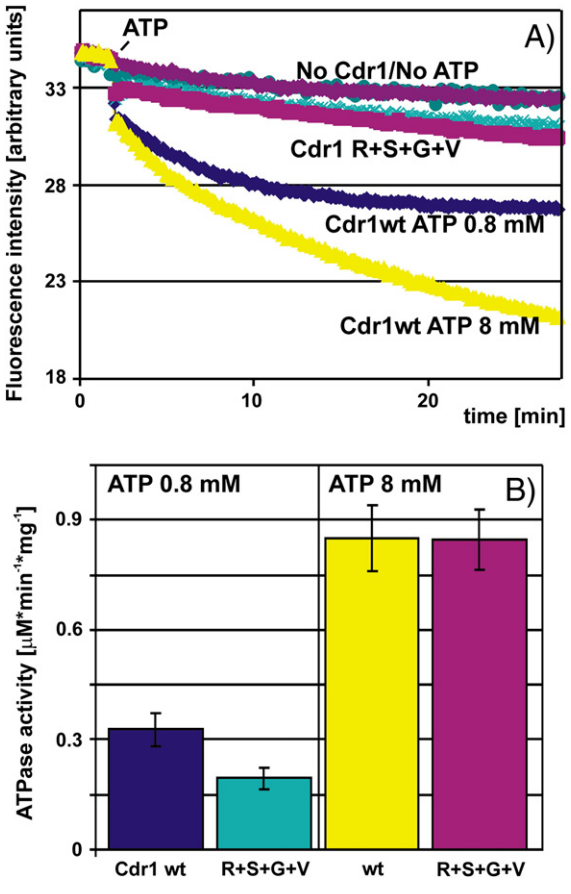


**Fig. 8.** $DiOC_6$ transport (A) and ATP hydrolysis (B) by the wild type and mutant Cdr1p in isolated plasma membranes. Membranes were isolated as described in Materials and methods. Drug transport and ATPase activities were measured at 30 °C, pH 7.5 in the presence of either 0.8 mM or 8 mM Mg-ATP and 12.5 mM azide, as described in Materials and methods.

## 4. Discussion

The pathways of intramolecular communication between the two nucleotide binding and transmembrane domains, arranged around a two-fold symmetry axis in the tertiary structures of ABC transporters, and their effect on substrate specificity are poorly understood.

To address this issue we combined the extensive knowledge of the multidrug detoxification system of the yeast *S. cerevisiae* with the ease of genetic manipulation in this model organism. We took a new approach and directed the evolution of one transporters specificity towards that of the other, exploiting the previously identified differences in the drug resistance profiles of the major MDR transporters Pdr5p and Snq2p of *S. cerevisiae* and Cdr1p of the pathogenic yeast *C. albicans*, members of the PDR subfamily of ABC transporters.

These proteins that evolved to handle a vast array of structurally unrelated molecules are a good model for the analysis of mechanisms of substrate translocation by MDR ABC transporters, as they share high sequence identity, which approaches 56% between Pdr5p and Cdr1p, 42% between Cdr1p and Snq2p and 37% between Pdr5p and Snq2p [72–75]. This is reflected by the corresponding degree of overlap in the substrate specificity profiles. These are in stark contrast to the majority of other transporters and enzymes, which usually show a narrow specificity for individual or closely related molecules. Studies in these systems pointed out to the importance of long distance amino acid interactions for substrate selection. In serine proteases, such as trypsin and chymotrypsin the specificity of catalysis has been shown to depend on the interaction with distal surface loops that affect the conformation of amino acids forming direct contacts with the substrates [28,29]. These interactions have been shown to be mediated by sparse networks of intermediary residues that are not evident even from the 3D structures, and are important for allosteric communication [42,76]. We hypothesized that the directed evolution approach targeted at substrate profile alteration could therefore point out new residues important for intramolecular communication in the PDR subfamily of ABC transporters.

In support of this hypothesis, our screen based on positive selection of Cdr1p mutants conferring increased resistance to Snq2p substrate resazurine, identified mutations specifically clustered in each domain of the protein. The two pairs of mutations were roughly pseudosymmetrically located (Fig. 1) in relation to the two fold rotational symmetry axis typically observed in three dimensional reconstructions of ABC MDR transporters, including the low resolution Pdr5p structure [17,53,61,77,78]. We believe that this characteristic and functionally important pattern of mutations was revealed thanks to the gain of function selection procedure and saturation of the screen suggested by hitting the same sites in multiple independent clones. The positive selection allowed to intrinsically eliminate the nonfunctional, poorly expressed or incorrectly processed mutants, contributing to much higher heterogeneity observed previously in a few other global screens [35,79] employing negative selection for loss of resistance. Interestingly symmetric interfaces are common to form two-state conformational switches, and mutations affecting allosteric communication in several ligand-gated channels [80–82] were often found located close to the symmetry axes, which is in line with the proposed mechanisms of allosteric signal transduction [83].

Several lines of evidence indicate an important role of the newly identified residues in interdomain communication, its link with substrate specificity and reveal conserved features within different subfamilies of ABC transporters.

Our mutants significantly differ from those point mutants, previously identified within the PDR subfamily, with defects in ATP hydrolysis or binding as all of them reported so far conferred a decreased level of resistance to the tested drug substrates. In particular none of the mutants of this type has been shown to mediate increased drug resistance or transport. In contrast our novel class of mutants showed selective alterations in specificity including increased capability to transport some of Snq2p substrates. These include the resorufin derivatives, as revealed by the newly developed assay of resorufin acetate transport. A parallel drastic reduction of resistance was observed for selected azoles, such as itraconazole in the C363R and G521S/D mutants, the effect increasing with the size and polarity of residue 521, the latter being also more sensitive to fenbuconazole. Only minor changes in resistance to some compounds such as cycloheximide or fluconazole, selective for Pdr5p and Cdr1p, were seen.

The stable high level overproduction achieved for the heterologous MDR transporter Cdr1p in a strain devoid of the major endogenous efflux pumps *PDR5*, *SNQ2* and *YOR1*, reduced the background of endogenous activities and increased the accuracy of the functional characterization of mutants. These were overproduced at the level comparable to the wild type protein as determined by two independent approaches, and located correctly to the plasma membrane, demonstrating that the large differences in drug resistance and transport result from the functional alterations of the proteins, rather than from differences in the expression level or mislocalization.

Given the lack of Cdr1p structural information, to gain insight into the relative location of the mutations, their positions have been mapped onto the available three dimensional structures of ABC transporters NBDs using structure based alignment. This approach was validated by the relatively high sequence conservation of these cytosolic regions and the fact that the tertiary structures are generally much better conserved than the corresponding sequences. Analysis of the available structures of complete MDR transporters indicated that the mutated regions in both NBDs as well as in central parts of TM helix 1 and 7 are far apart. Thus the strong synergistic effects on drug transport and resistance as well as the drug dependent ATPase activity revealed by double mutant analysis, must result from long distance allosteric interactions between the identified residues. Their role in interdomain communication was also suggested by SCA, supported by analysis of available mutational data in multiple subfamilies of ABC transporters. The observed pseudosymmetry of the intramolecular interaction network in Cdr1p reflected the pseudosymmetrical location of the newly identified mutations and the observations of others [18,59,33]. V885 was identified as part of the larger cluster of interacting residues (Fig. 6C), that included the TM helix 7 residue L1209, being in direct contact with the preceding A1208 identified in our screen. It is likely that the selection conditions for increased resazurine resistance required a change in this neighboring residue to allow for more subtle changes in drug specificity. A reminiscent situation has been observed with disease causing mutations in several human proteins, which omitted the critical for function coevolving residues, and located in their immediate surrounding modulating their function through direct contacts [84]. Another possibility may be related to the inherent sensitivity of coevolution detecting algorithms to the conservation level of amino acids in each column of the multiple sequence alignment [85]. Additional limits are imposed by the clustering algorithms which allow the allocation of a given residue to only one cluster. Given the large size of ABC transporters and the complexity of the coordinated interdomain interactions, required for completion of the transport cycle energized by ATP hydrolysis, it is likely that the interaction network sampled by the SCA approach is underrepresented.

Nevertheless the high predictive power of SCA has previously been documented experimentally in several protein families of smaller size [42,56]. The validity of our approach is further supported by the fact that many residues evolutionarily related to V885 (Fig. 6C) located within or in close contact with the highly mobile regions, previously shown by molecular dynamics simulations to undergo extensive rearrangements during the catalytic cycle of ABC transporters. This is in line with the observations of others that the coevolving residues cluster in flexible regions of proteins involved in allosteric communication [86–88]. These regions include the X-loop, A-loop, the loop between alpha helices 3 and 4 of the signaling subdomain of NBD2 and loops connecting the transmembrane helices [53,57–61]. In addition the SCA analysis of Cdr1p was in agreement with the available mutagenesis data not only on members of the PDR subfamily, including the recent reports on intramolecular communication in Pdr5p [32,33], but also with numerous data from other groups of ABC transporters, including P-glycoprotein. Interestingly the X-loop region, predicted to communicate with the Walker A preceding V885 in Cdr1p, has previously been shown to be involved in the control of substrate specificity of the mouse Mdr3 [89], supporting its role in signal transmission to the TMDs. Several other observations point out to the important and evolutionarily conserved role for the Walker A preceding region, corresponding to V885 of Cdr1p in communication between the NBD and TMD domains in multiple ABC transporter subfamilies, including exporters of inverted topologies, importers and the CFTR $Cl^-$ channel.

Interestingly residues corresponding to V885 of Cdr1p, mapping at the end of strand 2 of the catalytic subdomain of NBD2 make conserved contact with the region preceding the H-loop in the structures of several NBDs of ABC transporters. This is shown in Fig. 9 for the

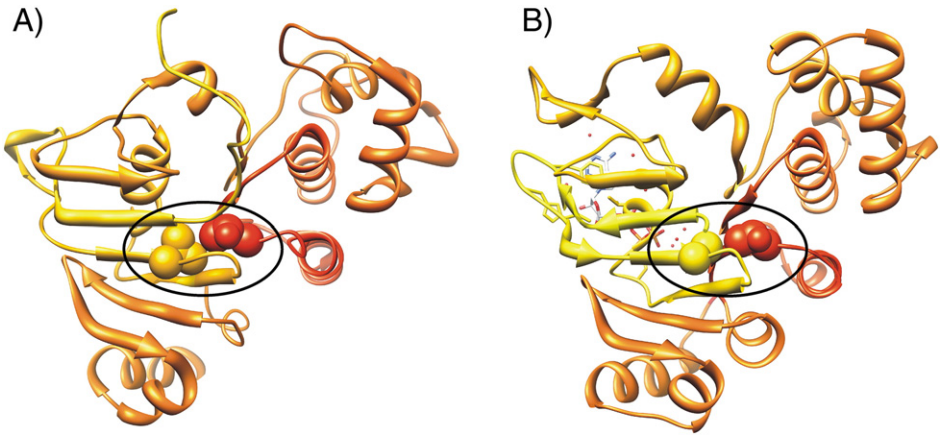


**Fig. 9.** Mapping the position of V885 of Cdr1p onto the structure of mouse P-gp (3G60) (A), and HisP (1B0U) (B), reveals a conservation of the close contact of the corresponding residues V1056 of P-gp and A29 of HisP, respectively with the strand preceding the H-loop (residues T1222 of P-gp, and T205 of HisP).

mouse P-gp (residues V1056 and T1222 of NBD2) and His-P (residues A29 and T205). A similar contact was observed between the symmetrically located, corresponding residues V413 and T577 in the opposite NBD1 of the mouse mdr3 P-gp.

Recent molecular dynamics simulations revealed this region as an anchor and pivot for the preceding helix D of the helical subdomain [90]. Movements of helix D occurred in concert with residues located in the D-loop on its opposite side as well as motive C, which follows immediately the X loop. The region preceding the H-loop has previously been shown to communicate with, and affect the function of the transmembrane domains in both HisP and P-gp. Substitution T205M of His P enabled the uptake of histidine in the absence of the otherwise indispensable substrate binding protein HisJ [91], whereas T205A suppressed the effect of the HisJ mutation which inactivated its domain responsible for interaction with the transmembrane region of the transporter. Alteration of the drug resistance profile was a consequence of the T578C mutation in the mouse mdr3 P-glycoprotein [89]. This residue remaining in close contact with T577 and separated by four amino acids from the conserved His of the H-loop in NBD1, is located symmetrically to the corresponding C1223 of NBD2 and in the alignment follows T205 of HisP. Finally this region in the NBD1 of yeast Pdr5p (T363 corresponding to I579 of the mouse mdr3 P-glycoprotein) has been recovered as a partial suppressor of L183P (which corresponds to V413 of P-gp, A29 of HisP, and M177 of Cdr1p- in the location corresponding to V885 but in the opposite NBD1 domain) which resulted in the endoplasmic reticulum retention of the protein [92]. These contacts are of particular interest, in light of the recent observation that a mutation H1068A of the conserved histidine, defining the H-loop of Pdr5p NBD2, selectively affected substrate specificity [73]. This was also the case for the identified C363R substitution in the pseudosymmetrically located region of the opposite NBD1 of Cdr1p that appeared functionally coupled to V885 in the double mutant analysis. These observations further confirm the conserved nature of the influence of the Walker A preceding region and V885 of Cdr1p and its corresponding residues on the status of transmembrane domains in a diverse range of ABC transporters, pointing out to the importance of the H-loop region in this process. Of note is also the fact that the H-loop and X loop regions have been revealed as important, disease associated structural hotspots in human ABC transporters [93].

The S1235R substitution in CFTR, a unique member of the ABC superfamily serving as a chloride channel which when malfunctions is associated with mucoviscidosis may lead to symptoms of varying degrees when heterozygous with other more severe mutations. This location corresponding to K886 of Cdr1p, a residue next to and in direct contact with V885 identified in our mutagenesis screen, affected the functional properties of the transmembrane domains, increasing the open probability of the chloride channel [94].

Given the effect observed in CFTR it is likely that the altered resistance profile of the V885G and the identified functionally related substitutions could result from changes in the dynamics or range of motions of the transmembrane helices, which would be in line with the model of kinetic substrate selection proposed by Ernst et al. [67]. It assumes that modifications of drug specificity may result from changes in the equilibration time of transported substrates with the drug binding site which depend on the kinetics of conformational changes. Interestingly an altered kinetics of CFTR channel was also a result of mutations in residues predicted to directly interact with the adenine ring of ATP and the central part of TM helix 6 [95,96]. Thus the large increase of the $K_M$ for ATP hydrolysis of the quadruple C363R, G521S, V885G, A1208V Cdr1p mutant is likely to be associated with the altered kinetics of transport related conformational changes resulting in profound changes in the drug resistance profile and markedly reduced resistance and transport mediated by this allele. This would be consistent with the drug and mutation selective effects on ATPase activity and the marked hypersensitivity of the quadruple mutant to fenbuconazole inhibition, indicating maintenance of some sort of interdomain communication even in this transport compromised mutant.

In line with this, the increasing polarity of residues in the TM helices, which is the case of the identified G521S and D substitutions, has been shown previously to promote formation of interhelical hydrogen bonds in CFTR and P-glycoprotein and alter, as a consequence, the alignment and movements of the TM helices associated with modification of substrate specificity [97,98]. As glycine and alanine residues have an important role in mediating TM helix interactions and occur at an increased frequency at helix crossing points [99,100], a similar consequence may result from the substitution of A1208 by the more bulky V. Of note is a role of the G185V mutation in TM helix 3 of human P-glycoprotein, suggested as a pivotal point in the communication between drug and nucleotide binding domains and resulting in a more efficient transport of colchicine [64].

Altogether mutational data in multiple subfamilies of ABC transporters combined with the functional and SCA analysis of the newly identified Cdr1p residues suggest their important and conserved role in communication between the NB and TM domains.

Our results contribute towards better understanding of the intramolecular communication within ABC superfamily proteins, which is of vital importance for the understanding of their mechanism of action and substrate selectivity, as well as for a better control of multidrug resistance phenomena in the clinical setting.

## Acknowledgments

This work was supported in part by grants from the Ministry of Science and Higher Education (2P05A 080 28 and funds for the Wroclaw Medical University). We thank J. Otlewski, A. Polanowski, J. Gutowicz and A. Sikorski for sharing laboratory equipment, G. Getz, E. Levine and E. Domany for sharing the CTWC application and K.Y. Yip for sharing the Coevolution system and helpful comment.

## References

[1] I.B. Holland, M.A. Blight, ABC-ATPases, adaptable energy generators fuelling transmembrane movement of a variety of molecules in organisms from bacteria to humans, J. Mol. Biol. 293 (1999) 381–399.
[2] A.L. Davidson, E. Dassa, C. Orelle, J. Chen, Structure, function, and evolution of bacterial ATP-binding cassette systems, Microbiol. Mol. Biol. Rev. 72 (2008) 317–364.
[3] R.D. Cannon, E. Lamping, A.R. Holmes, K. Niimi, P.V. Baret, M.V. Keniya, K. Tanabe, M. Niimi, A. Goffeau, B.C. Monk, Efflux-mediated antifungal drug resistance, Clin. Microbiol. Rev. 22 (2009) 291–321.
[4] G. Szakács, J.K. Paterson, J.A. Ludwig, C. Booth-Genthe, M.M. Gottesman, Targeting multidrug resistance in cancer, Nat. Rev. Drug Discov. 5 (2006) 219–234.
[5] A.R. Holmes, Y.H. Lin, K. Niimi, E. Lamping, M. Keniya, M. Niimi, K. Tanabe, B.C. Monk, R.D. Cannon, ABC transporter Cdr1p contributes more than Cdr2p does to fluconazole efflux in fluconazole-resistant *Candida albicans* clinical isolates, Antimicrob. Agents Chemother. 52 (2008) 3851–3862.
[6] M. Kolaczkowski, A. Kolaczkowska, J. Luczynski, S. Witek, A. Goffeau, In vivo characterization of the drug resistance profile of the major ABC transporters and other components of the yeast pleiotropic drug resistance network, Microb. Drug Resist. 4 (1998) 143–158.
[7] E. Lamping, P.V. Baret, A.R. Holmes, B.C. Monk, A. Goffeau, R.D. Cannon, Fungal PDR transporters: phylogeny, topology, motifs and function, Fungal Genet. Biol. 47 (2010) 127–142.
[8] A. Kovalchuk, A.J. Driessen, Phylogenetic analysis of fungal ABC transporters, BMC Genomics 11 (Mar 16 2010) 177.
[9] A. Decottignies, A. Goffeau, Complete inventory of the yeast ABC proteins, Nat. Genet. 15 (1997) 137–145.
[10] M.H. Saier Jr., A functional-phylogenetic classification system for transmembrane solute transporters, Microbiol. Mol. Biol. Rev. 64 (2000) 354–411.
[11] B. Rogers, A. Decottignies, M. Kolaczkowski, E. Carvajal, E. Balzi, A. Goffeau, The pleiotropic drug ABC transporters from *Saccharomyces cerevisiae*, J. Mol. Microbiol. Biotechnol. 3 (2001) 207–214.
[12] J. Crouzet, T. Trombik, A.S. Fraysse, M. Boutry, Organization and function of the plant pleiotropic drug resistance ABC transporter family, FEBS Lett. 580 (2006) 1123–1130.
[13] M. Gaur, D. Choudhury, R. Prasad, Complete inventory of ABC proteins in human pathogenic yeast, *Candida albicans*, J. Mol. Microbiol. Biotechnol. 9 (2005) 3–15.
[14] D. Taglicht, S. Michaelis, *Saccharomyces cerevisiae* ABC proteins and their relevance to human health and disease, Methods Enzymol. 292 (1998) 130–162.
[15] G.E. Tusnády, B. Sarkadi, I. Simon, A. Váradi, Membrane topology of human ABC proteins, FEBS Lett. 580 (2006) 1017–1022.
[16] E. Biemans-Oldehinkel, M.K. Doeven, B. Poolman, ABC transporter architecture and regulatory roles of accessory domains, FEBS Lett. 580 (2006) 1023–1035.

[17] A. Ferreira-Pereira, S. Marco, A. Decottignies, J. Nader, A. Goffeau, J.L. Rigaud, Three-dimensional reconstruction of the *Saccharomyces cerevisiae* multidrug resistance protein Pdr5p, J. Biol. Chem. 278 (2003) 11995–11999.

[18] A. Kumar, S. Shukla, A. Mandal, S. Shukla, S.V. Ambudkar, R. Prasad, Divergent signature motifs of nucleotide binding domains of ABC multidrug transporter, CaCdr1p of pathogenic *Candida albicans*, are functionally asymmetric and non-interchangeable, Biochim. Biophys. Acta 1798 (2010) 1757–1766.

[19] M. Chen, R. Abele, R. Tampé, Functional non-equivalence of ATP-binding cassette signature motifs in the transporter associated with antigen processing (TAP), J. Biol. Chem. 279 (2004) 46073–46081.

[20] C. Basso, P. Vergani, A.C. Nairn, D.C. Gadsby, Prolonged nonhydrolytic interaction of nucleotide with CFTR's $NH_2$-terminal nucleotide binding domain and its role in channel gating, J. Gen. Physiol. 122 (2003) 333–348.

[21] Y. Hou, L. Cui, J.R. Riordan, X. Chang, Allosteric interactions between the two non-equivalent nucleotide binding domains of multidrug resistance protein MRP1, J. Biol. Chem. 275 (2000) 20280–20287.

[22] R. Yang, L. Cui, Y.X. Hou, J.R. Riordan, X.B. Chang, ATP binding to the first nucleotide binding domain of multidrug resistance-associated protein plays a regulatory role at low nucleotide concentration, whereas ATP hydrolysis at the second plays a dominant role in ATP-dependent leukotriene C4 transport, J. Biol. Chem. 278 (2003) 30764–30771.

[23] M. Matsuo, N. Kioka, T. Amachi, K. Ueda, ATP binding properties of the nucleotide-binding folds of SUR1, J. Biol. Chem. 274 (1999) 37479–37482.

[24] K. Ueda, M. Matsuo, K. Tanabe, K. Morita, N. Kioka, T. Amachi, Comparative aspects of the function and mechanism of SUR1 and MDR1 proteins, Biochim. Biophys. Acta 1461 (1999) 305–313.

[25] A.E. Senior, M.K. al-Shawi, I.L. Urbatsch, The catalytic cycle of P-glycoprotein, FEBS Lett. 377 (1995) 285–289.

[26] Z.E. Sauna, M.M. Smith, M. Müller, K.M. Kerr, S.V. Ambudkar, The mechanism of action of multidrug-resistance-linked P-glycoprotein, J. Bioenerg. Biomembr. 33 (2001) 481–491.

[27] C.A. Hrycyna, M. Ramachandra, U.A. Germann, P.W. Cheng, I. Pastan, M.M. Gottesman, Both ATP sites of human P-glycoprotein are essential but not symmetric, Biochemistry 38 (1999) 13887–13899.

[28] L. Hedstrom, L. Szilagyi, W.J. Rutter, Converting trypsin to chymotrypsin, the role of surface loops, Science 255 (1992) 1249–1253.

[29] J.J. Perona, L. Hedstrom, W.J. Rutter, R.J. Fletterick, Structural origins of substrate discrimination in trypsin and chymotrypsin, Biochemistry 34 (1995) 1489–1499.

[30] L. Hedstrom, Trypsin, a case study in the structural determinants of enzyme specificity, Biol. Chem. 377 (1996) 465–470.

[31] P.A. Patten, N.S. Gray, P.L. Yang, C.B. Marks, G.J. Wedemayer, J.J. Boniface, R.C. Stevens, P.G. Schultz, The immunological evolution of catalysis, Science 271 (1996) 1086–1091.

[32] Z.E. Sauna, S. Supernavage Bohn, R. Rutledge, M.P. Dougherty, S. Cronin, L. May, D. Xia, S.V. Ambudkar, J. Golin, Mutations define cross-talk between the N-terminal nucleotide-binding domain and transmembrane helix-2 of the yeast multidrug transporter Pdr5, J. Biol. Chem. 283 (2008) 35010–35022.

[33] N. Ananthaswamy, R. Rutledge, Z.E. Sauna, S.V. Ambudkar, E. Dine, E. Nelson, D. Xia, J. Golin, The signaling interface of the yeast multidrug transporter Pdr5 adopts a cis conformation, and there are functional overlap and equivalence of the deviant and canonical Q-loop residues, Biochemistry 49 (2010) 4440–4449.

[34] M. Kolaczkowski, A. Kolaczkowska, N. Motohashi, K. Michalak, New high-throughput screening assay to reveal similarities and differences in inhibitory sensitivities of multidrug ATP-binding cassette transporters, Antimicrob. Agents Chemother. 53 (2009) 1516–1527.

[35] R. Egner, F.E. Rosenthal, A. Kralli, D. Sanglard, K. Kuchler, Genetic separation of FK506 susceptibility and drug transport in the yeast Pdr5 ATP-binding cassette multidrug resistance transporter, Mol. Biol. Cell 9 (1998) 523–543.

[36] F. Sanger, G.G. Nicklen, A.R. Coulson, DNA sequencing with chain terminating inhibitors, Proc. Natl. Acad. Sci. U. S. A. 74 (1977) 5463–5467.

[37] J.P. Dufour, A. Amory, A. Goffeau, Plasma membrane ATPase from the yeast *Schizosaccharomyces pombe*, Methods Enzymol. 157 (1988) 513–528.

[38] M. Kolaczkowski, M. van der Rest, A. Cybularz-Kolaczkowska, J.P. Soumillion, W.N. Konings, A. Goffeau, Anticancer drugs, ionophoric peptides, and steroids as substrates of the yeast multidrug transporter Pdr5p, J. Biol. Chem. 271 (1996) 31543–31548.

[39] D.J. Katzmann, E.A. Epping, W.S. Moye-Rowley, Mutational disruption of plasma membrane trafficking of *Saccharomyces cerevisiae* Yor1p, a homologue of mammalian multidrug resistance protein, Mol. Cell. Biol. 19 (1999) 2998–3009.

[40] S.W. Lockless, R. Ranganathan, Evolutionarily conserved pathways of energetic connectivity in protein families, Science 286 (1999) 295–299.

[41] K.Y. Yip, P. Patel, P.M. Kim, D.M. Engelman, D. McDermott, M. Gerstein, An integrated system for studying residue coevolution in proteins, Bioinformatics 24 (2008) 290–292.

[42] G.M. Suel, S.W. Lockless, M.A. Wall, R. Ranganathan, Evolutionarily conserved networks of residues mediate allosteric communication in proteins, Nat. Struct. Biol. 10 (2003) 59–69.

[43] M. Blatt, S. Wiseman, E. Domany, Superparamagnetic clustering of data, Phys. Rev. Lett. 76 (1996) 3251–3254.

[44] G. Getz, E. Levine, E. Domany, Coupled two-way clustering analysis of gene microarray data, Proc. Natl. Acad. Sci. U. S. A. 97 (2000) 12079–12084.

[45] A.J. Saldanha, Java Treeview — extensible visualization of microarray data, Bioinformatics 20 (2004) 3246–3248.

[46] A.I. Saeed, V. Sharov, J. White, J. Li, W. Liang, N. Bhagabati, J. Braisted, M. Klapa, T. Currier, M. Thiagarajan, A. Sturn, M. Snuffin, A. Rezantsev, D. Popov, A. Ryltsov, E. Kostukovich, I. Borisovsky, Z. Liu, A. Vinsavich, V. Trush, J. Quackenbush, TM4, a free, open-source system for microarray data management and analysis, Biotechniques 34 (2003) 374–378.

[47] R.C. Edgar, MUSCLE, multiple sequence alignment with high accuracy and high throughput, Nucleic Acids Res. 32 (2004) 1792–1797.

[48] F. Armougom, S. Moretti, O. Poirot, S. Audic, P. Dumas, B. Schaeli, V. Keduas, C. Notredame, Expresso, automatic incorporation of structural information in multiple sequence alignments using 3D-Coffee, Nucleic Acids Res. 34 (2006) W604–W608.

[49] G. Pollastri, A. McLysaght, Porter, a new, accurate server for protein secondary structure prediction, Bioinformatics 21 (2005) 1719–1720.

[50] D. Juretić, L. Zoranić, D. Zucić, Basic charge clusters and predictions of membrane protein topology, J. Chem. Inf. Comput. Sci. 42 (2002) 620–632.

[51] E.F. Pettersen, T.D. Goddard, C.C. Huang, G.S. Couch, D.M. Greenblatt, E.C. Meng, T.E. Ferrin, UCSF Chimera — a visualization system for exploratory research and analysis, J. Comput. Chem. 25 (2004) 1605–1612.

[52] C. Oswald, I.B. Holland, L. Schmitt, The motor domains of ABC-transporters. What can structures tell us? Naunyn Schmiedebergs Arch. Pharmacol. 372 (2006) 385–399.

[53] R.J. Dawson, K.P. Locher, Structure of a bacterial multidrug ABC transporter, Nature 443 (2006) 180–185.

[54] T. Miyama, H. Takanaga, H. Matsuo, K. Yamano, K. Yamamoto, T. Iga, M. Naito, T. Tsuruo, H. Ishizuka, Y. Kawahara, Y. Sawada, P-glycoprotein-mediated transport of itraconazole across the blood–brain barrier, Antimicrob. Agents Chemother. 42 (1998) 1738–1744.

[55] M. Takano, R. Hasegawa, T. Fukuda, R. Yumoto, J. Nagai, T. Murakami, Interaction with P-glycoprotein and transport of erythromycin, midazolam and ketoconazole in Caco-2 cells, Eur. J. Pharmacol. 358 (1998) 289–294.

[56] Y. Chen, K. Reilly, Y. Chang, Evolutionarily conserved allosteric network in the Cys loop family of ligand-gated ion channels revealed by statistical covariance analyses, J. Biol. Chem. 281 (2006) 18184–18192.

[57] J.P. Becker, F. Van Bambeke, P.M. Tulkens, M. Prevost, Dynamics and structural changes induced by ATP binding in Sav 1866, a bacterial ABC exporter, J. Phys. Chem. B 114 (2010) 15948–15957.

[58] J.M. Damas, A.S. Oliveira, A.M. Baptista, C.M. Soares, Structural consequences of ATP hydrolysis on the ABC transporter NBD dimer, molecular dynamics studies of Hly-B, Protein Sci. 20 (2011) 1220–1230.

[59] J. Aittoniemi, H. de Wet, F.M. Ashcroft, M.S. Sansom, Asymmetric switching in a homodimeric ABC transporter: a simulation study, PLoS Comput. Biol. 6 (2010) e1000762.

[60] P.M. Jones, A.M. George, Opening of the ADP-bound active site in the ABC transporter ATPase dimer, evidence for a constant contact, alternating sites model for the catalytic cycle, Proteins 75 (2009) 387–396.

[61] A. Ward, C.L. Reyes, J. Yu, C.B. Roth, G. Chang, Flexibility in the ABC transporter MsbA: alternating access with a twist, Proc. Natl. Acad. Sci. U. S. A. 104 (2007) 19005–19010.

[62] G.F. Ames, K. Nikaido, I.X. Wang, P.Q. Liu, C.E. Liu, C. Hu, Purification and characterization of the membrane-bound complex of an ABC transporter, the histidine permease, J. Bioenerg. Biomembr. 33 (2001) 79–92.

[63] M.K. Al-Shawi, M.K. Polar, H. Omote, R.A. Figler, Transition state analysis of the coupling of drug transport to ATP hydrolysis by P-glycoprotein, J. Biol. Chem. 278 (2003) 52629–52640.

[64] H. Omote, R.A. Figler, M.K. Polar, M.K. Al-Shawi, Improved energy coupling of human P-glycoprotein by the glycine 185 to valine mutation, Biochemistry 43 (2004) 3917–3928.

[65] A. Decottignies, M. Kolaczkowski, E. Balzi, A. Goffeau, Solubilization and characterization of the overexpressed PDR5 multidrug resistance nucleotide triphosphatase of yeast, J. Biol. Chem. 269 (1994) 12797–12803.

[66] J. Golin, Z.N. Kon, C.P. Wu, J. Martello, L. Hanson, S. Supernavage, S.V. Ambudkar, Z.E. Sauna, Complete inhibition of the Pdr5p multidrug efflux pump ATPase activity by its transport substrate clotrimazole suggests that GTP as well as ATP may be used as an energy source, Biochemistry 46 (2007) 13109–13119.

[67] R. Ernst, P. Kueppers, C.M. Klein, T. Schwarzmueller, K. Kuchler, L. Schmitt, A mutation of the H-loop selectively affects rhodamine transport by the yeast multidrug ABC transporter Pdr5, Proc. Natl. Acad. Sci. U. S. A. 105 (2008) 5069–5074.

[68] M.H. Toivari, A. Aristidou, L. Ruohonen, M. Penttila, Conversion of xylose to ethanol by recombinant *Saccharomyces*, Metab. Eng. 3 (2001) 236–249.

[69] A. Nilsson, I.L. Pahlman, P.A. Jovall, A. Blomberg, C. Larsson, L. Gustafsson, The catabolic capacity of *Saccharomyces cerevisiae*, Yeast 18 (2001) 1371–1381.

[70] R.M. Wadkins, P.J. Houghton, Kinetics of transport of dialkyloxacarbocyanines in multidrug-resistant cell lines overexpressing P-glycoprotein: interrelationship of dye alkyl chain length, cellular flux, and drug resistance, Biochemistry 34 (1995) 3858–3872.

[71] A. Kolaczkowska, M. Kolaczkowski, A. Goffeau, W.S. Moye-Rowley, Compensatory activation of the multidrug transporters Pdr5p, Snq2p, and Yor1p by Pdr1p in *Saccharomyces cerevisiae*, FEBS Lett. 582 (2008) 977–983.

[72] J. Servos, E. Haase, M. Brendel, Gene SNQ2 of *Saccharomyces cerevisiae*, which confers resistance to 4-nitroquinoline-N-oxide and other chemicals, encodes a 169 kDa protein homologous to ATP-dependent permeases, Mol. Gen. Genet. 236 (1993) 214–218.

[73] E. Balzi, M. Wang, S. Leterme, L. van Dyck, A. Goffeau, PDR5, a novel yeast multidrug resistance conferring transporter controlled by the transcription regulator *PDR1*, J. Biol. Chem. 269 (1994) 2206–2214.

[74] P.H. Bissinger, K. Kuchler, Molecular cloning and expression of the *Saccharomyces cerevisiae STS1* gene product. A yeast ABC transporter conferring mycotoxin resistance, J. Biol. Chem. 269 (1994) 4180–4186.

[75] R. Prasad, P. de Wergifosse, A. Goffeau, E. Balzi, Molecular cloning and characterization of a novel gene of *Candida albicans*, *CDR1*, conferring multiple resistance to drugs and antifungals, Curr. Genet. 27 (1995) 320–329.

[76] J. Lee, M. Natarajan, V.C. Nashine, M. Socolich, T. Vo, W.P. Russ, S.J. Benkovic, R. Ranganathan, Surface sites for engineering allosteric control in proteins, Science 322 (2008) 438–442.
[77] S.G. Aller, J. Yu, A. Ward, Y. Weng, S. Chittaboina, R. Zhuo, P.M. Harrell, Y.T. Trinh, Q. Zhang, I.L. Urbatsch, G. Chang, Structure of P-glycoprotein reveals a molecular basis for poly-specific drug binding, Science 323 (2009) 1718–1722.
[78] R.M. Rutledge, L. Esser, J. Ma, D. Xia, Toward understanding the mechanism of action of the yeast multidrug resistance transporter Pdr5p: a molecular modeling study, J. Struct. Biol. 173 (2011) 333–344.
[79] A.C. Tutulan-Cunita, M. Mikoshi, M. Mizunuma, D. Hirata, T. Miyakawa, Mutational analysis of the yeast multidrug resistance ABC transporter Pdr5p with altered drug specificity, Genes Cells 10 (2005) 409–420.
[80] J.L. Galzi, S.J. Edelstein, J. Changeux, The multiple phenotypes of allosteric receptor mutants, Proc. Natl. Acad. Sci. U. S. A. 93 (1996) 1853–1858.
[81] Y. Chang, D.S. Weiss, Allosteric activation mechanism of the $\alpha_1\beta_2\gamma_2$ γ-aminobutyric acid type A receptor revealed by mutation of the conserved M2 leucine, Biophys. J. 77 (1999) 2542–2551.
[82] C. Grosman, A. Auerbach, Kinetic, mechanistic, and structural aspects of unliganded gating of acetylcholine receptor channels, A single-channel study of second transmembrane segment 12′ mutants, J. Gen. Physiol. 115 (2000) 621–635.
[83] J.P. Changeux, S.J. Edelstein, Allosteric mechanisms of signal transduction, Science 308 (2005) 1424–1428.
[84] A. Kowarsch, A. Fuchs, D. Frishman, P. Pagel, Correlated mutations: a hallmark of phenotypic amino acid substitutions, PLoS Comput. Biol. 6 (2010) e1000923.
[85] A.A. Fodor, R.W. Aldrich, Influence of conservation on calculations of amino acid covariance in multiple sequence alignments, Proteins 56 (2004) 211–221.
[86] J. Jeon, H. Nam, Y.S. Choi, J. Yang, J. Hwang, S. Kim, Molecular evolution of protein conformational changes revealed by a network of evolutionarily coupled residues, Mol. Biol. Evol. 28 (2011) 2675–2685.
[87] H. Shen, F. Xu, H. Hu, F. Wang, Q. Wu, Q. Huang, H. Wang, Coevolving residues of (b/a)8-barrel proteins play roles in stabilizing active site architecture and coordinating protein dynamics, J. Struct. Biol. 164 (2008) 281–292.
[88] S. Bruschweiler, P. Schanda, K. Kloiber, B. Brutscher, G. Kontaxis, R. Konrat, M. Tollinger, Direct observation of the dynamic process underlying allosteric signal transmission, J. Am. Chem. Soc. 131 (2009) 3063–3068.
[89] L. Beaudet, P. Gros, Functional dissection of P-glycoprotein nucleotide-binding domains in chimeric and mutant proteins. Modulation of drug resistance profiles, J. Biol. Chem. 270 (1995) 17159–17170.
[90] P.M. Jones, A.M. George, Role of the D-loops in allosteric control of ATP hydrolysis in an ABC transporter, J. Phys. Chem. (2012), http://dx.doi.org/10.1021/jp211139s.
[91] D.M. Speiser, G.F. Ames, *Salmonella typhimurium* histidine periplasmic permease mutations that allow transport in the absence of histidine-binding proteins, J. Bacteriol. 173 (1991) 1444–1451.
[92] C.P. de Thozée, S. Cronin, A. Goj, J. Golin, M. Ghislain, Subcellular trafficking of the yeast plasma membrane ABC transporter, Pdr5, is impaired by a mutation in the N-terminal nucleotide-binding fold, Mol. Microbiol. 63 (2007) 811–825.
[93] L. Kelly, H. Fukushima, R. Karchin, J.M. Gow, L.W. Chinn, U. Pieper, M.R. Segal, D.L. Kroetz, A. Sali, Functional hot spots in human ATP-binding cassette transporter nucleotide binding domains, Protein Sci. 19 (2010) 2110–2121.
[94] L. Wei, A. Vankeerberghen, M. Jaspers, J. Cassiman, B. Nilius, H. Cuppens, Suppressive interactions between mutations located in the two nucleotide binding domains of CFTR, FEBS Lett. 473 (2000) 149–153.
[95] Z. Zhou, X. Wang, H. Liu, X. Zou, M. Li, T. Hwang, The two ATP binding sites of the cystic fibrosis transmembrane conductance regulator (CFTR) play distinct roles in gating kinetics and energetics, J. Gen. Physiol. 128 (2006) 413–422.
[96] K. Jih, Y. Sohma, T. Hwang, Nonintegral stoichiometry in CFTR gating revealed by a pore-lining mutation, J. Gen. Physiol. (2012), http://dx.doi.org/10.1085/jgp.201210834.
[97] T.W. Loo, M.C. Bartlett, D.M. Clarke, Arginines in the first transmembrane segment promote maturation of a P-glycoprotein processing mutant by hydrogen bond interactions with tyrosines in transmembrane segment 11, J. Biol. Chem. 283 (2008) 24860–24870.
[98] A.G. Therien, F.E. Grant, C.M. Deber, Interhelical hydrogen bonds in the CFTR membrane domain, Nat. Struct. Biol. 8 (2001) 597–601.
[99] M.M. Javadpour, M. Eilers, M. Groesbeek, S.O. Smith, Helix packing in polytopic membrane proteins: role of glycine in transmembrane helix association, Biophys. J. 77 (1999) 1609–1618.
[100] M. Eilers, S.C. Shekar, T. Shieh, S.O. Smith, P.J. Fleming, Internal packing of helical membrane proteins, Proc. Natl. Acad. Sci. U. S. A. 97 (2000) 5796–5801.